bioRxiv preprint doi: https://doi.org/10.1101/094680; this version posted December 16, 2016. The copyright holder for this preprint (which was not certified by peer review) is the author/funder, who has granted bioRxiv a license to display the preprint in perpetuity. It is made available under aCC-BY-NC-ND 4.0 International license.

CORTICO-CORTICAL FEEDBACK CONTROLS SPATIAL SUMMATION IN PRIMATE VISUAL CORTEX

Lauri Nurminen[1]*, Sam Merlin[1]*, Maryam Bijanzadeh[1,2], Frederick Federer[1] and Alessandra Angelucci[1]

Author affiliations:

1) Department of Ophthalmology and Visual Science, Moran Eye Institute, University of Utah
2) Interdepartmental Program in Neuroscience, University of Utah
* Equal contribution

Corresponding author email addresses:
Lauri Nurminen, lauri.nurminen@utah.edu
Alessandra Angelucci, Alessandra.Angelucci@hsc.utah.edu

bioRxiv preprint doi: https://doi.org/10.1101/094680; this version posted December 16, 2016. The copyright holder for this preprint (which was not certified by peer review) is the author/funder, who has granted bioRxiv a license to display the preprint in perpetuity. It is made available under aCC-BY-NC-ND 4.0 International license.

Optogenetic inactivation of cortical feedback in primate visual cortex

ABSTRACT

Our visual perception of the external world relies on neural activity across a hierarchy of visual cortical areas, communicating via complex feedforward-feedback pathways. While feedforward pathways have been a focus of study, the role of the feedback pathway has remained poorly understood. Here we have developed a novel viral vector combination allowing for selective optogenetic inactivation of feedback pathways in the non-human primate brain. We show that even the most fundamental response properties of visual neurons, such as the receptive field size, are regulated by feedback signals from other regions of the visual cortex. Depending on its activity regime, cortico-cortical feedback can regulate receptive field size and contextual modulation of visual responses or the overall response gain of neurons.

INTRODUCTION

There has been major controversy regarding the causal contribution of cortico-cortical feedback projections to visual response properties of neurons in the primary visual cortex (V1); cooling of area MT [1], and cooling [2] or GABA inactivation [3] of V2 in anesthetized primates has produced general reductions in response gain with little or no effect on surround modulation. Simultaneous cooling of V2 and V3 in awake macaques has produced variable effects including increased or decreased responses and decreased surround modulation [4]. However, instead of specifically targeting feedback neurons, cooling and pharmacology affect an entire cortical area and therefore these methods may involve indirect pathways through thalamus or other cortical areas. Moreover, with these methods the level of inactivation cannot be controlled and thereby nuanced and physiologically more relevant manipulations have been difficult to achieve.

METHODS

By targeting optogenetic inactivation to feedback axons in primate V1, we have overcome the limitations of previous studies and show that feedback controls receptive field (RF) size, surround modulation and the response gain of V1 neurons. To achieve this, we developed a novel Cre-dependent viral vector combination, which allows for specific anterograde targeting of neural pathways. Separate viral vectors (AAV9.CaMKII.Cre, 3.7×10^{13} particles/ml, and AAV9.flex.CAG.ArchT-GFP, 9.8×10^{12}particles/ml, 1:1 mixture, Penn Vector Core, University of Pennsylvania, PA) carrying the genes for the outward proton pump ArchT [5] were mixed and injected into L2/3 and L6 of V2 guided by intrinsic signal optical imaging [6] (**Figure 1A**, 3 marmosets, 2-3 injection sites/animal, 240nl/site at 500µm depth for L2/3 and 1200µm depth for L6, 40-50µm tip diameter, 15 minutes/240nl [7]). This allows for selective and strong opsin expression in the axons of V2 feedback neurons in V1 (**Figure 1C**). Following 62-68 days transport, animals were anesthetized (induction: 30mg/kg ketamine i.m., surgery: 2% isoflurane in O_2, recording: 8-13µg/kg/hr sufentanil citrate i.v.), spike-rates to drifting sinusoidal gratings (100% contrast, 500ms presentation, 750ms ISI) of 66 visually responsive (response > 2SD above baseline) and stimulus modulated (one-way ANOVA $p<0.05$) V1 single-units were recorded (linear multielectrode array, V-Probe, Plexon; amplification, Cerebus, Blackrock Microsystems) while trial interleaved and balanced laser stimulation (532nm, 500ms pulse width, 2.8mm diameter collimated spot, 9-43 mW mm^{-2}, through thinned skull) was directed onto V2 feedback axons in V1 (spike-sorting with klusta [8, 9]). The recordings were targeted to opsin expressing regions of V1 with the aid of GFP-goggles (**Figure 1B**). Approximately 61% (40/66) of the visually driven single-units were modulated by the laser (two-way ANOVA, either laser or

bioRxiv preprint doi: https://doi.org/10.1101/094680; this version posted December 16, 2016. The copyright holder for this preprint (which was not certified by peer review) is the author/funder, who has granted bioRxiv a license to display the preprint in perpetuity. It is made available under aCC-BY-NC-ND 4.0 International license.

stimulus diameter x laser interaction, $p < 0.05$, or at least two successive data points significantly different to the same direction, $p_{bootstrap} < 0.05$). Heat may alter spiking in the cortex [10] and thus we selected safe range of light intensities for the inactivation experiments based on a control experiment without opsins (**Figure 1F**). All procedures conformed to the guidelines of the University of Utah Institutional Animal Care and Use Committee.

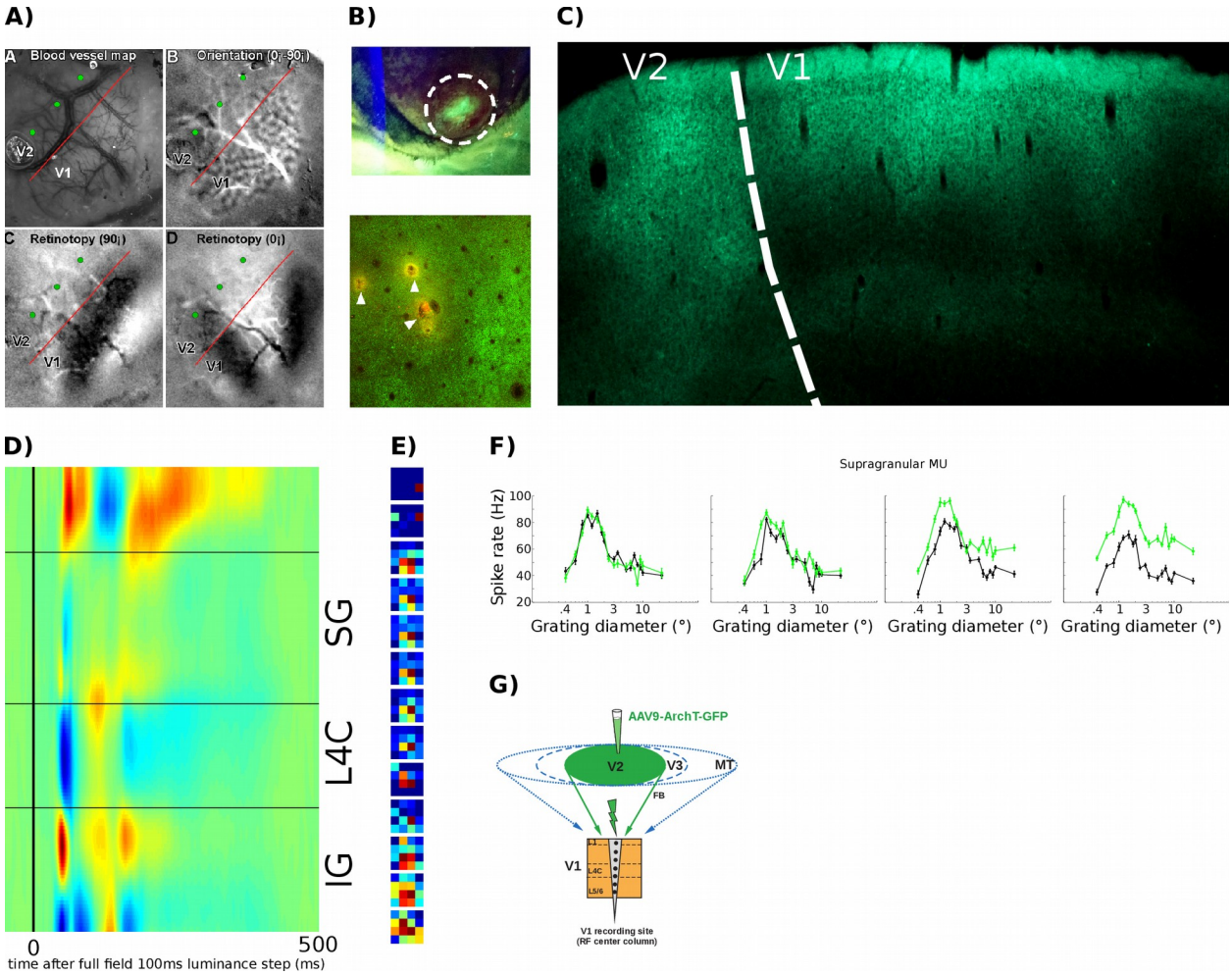

Figure 1. A novel viral vector combination enables specific anterograde expression of ArchT in feedback axons. A) Injections were guided with optical imaging of blood vessels (top left), orientation preference maps (top right) and retinotopic representations (bottom). **B)** Recordings were directed to regions of V1 expressing opsins. **top)** exposed V1 and V2 as seen through GPF-goggles, **bottom)** DiI marked electrode lesions (arrows) amid ArchT-GFP expressing axons in V1. **C)** ArchT-GFP expression is confined to axons in V1 while large number of V2 cells are labeled, confirming that the viral vector combination we have developed provides purely anterograde labeling. **D)** Borders of cortical layers were determined based on current source density analysis of evoked LFP signals to 100 ms luminance increment (0.5-100 cd m^{-2}) at every 400 ms (400 trials). SG (supragranular), IG (infragranular). **E)** Minimum response fields (mRF) were mapped with sparse noise. mRF alignment was used to ensure that the electrode array was inserted perpendicular to the surface of the brain. **F)** Control experiment without opsin determined the safe range of light intensities used in the inactivation experiment. SG multiunit (MU, continuous voltage recording thresholded at 5 times the noise standard deviation). **G)** Schematics of the inactivation paradigm. Light was shone on V2 feedback neuron axons in V1 while linear array recordings spanning all cortical layers were performed. Feedback from V2 is confined to the immediate vicinity of V1 neurons' receptive field (RF), termed the RF near-surround. Therefore, feedback inactivation is expected to modulate distal parts of the RF surround (RF far-surround) only modestly if at all.

bioRxiv preprint doi: https://doi.org/10.1101/094680; this version posted December 16, 2016. The copyright holder for this preprint (which was not certified by peer review) is the author/funder, who has granted bioRxiv a license to display the preprint in perpetuity. It is made available under aCC-BY-NC-ND 4.0 International license.

RESULTS

RF size is arguably one of the most fundamental properties of visual neurons and this study demonstrates, for the first time, that even such fundamental property is regulated by cortico-cortical feedback. The majority (76%) of the light-modulated single-units with well-defined RF showed an increase in their RF diameter (**Figure 2A, D**) when feedback from V2 was inactivated (15% showed no change and in 9% RF size decreased). The RF diameter was significantly smaller with intact feedback (1.27 ± 0.10º, all results reported as mean ± s.e.m.) compared to when feedback was optogenetically inactivated (1.83 ± 0.14º, $p_{bootstrap} < 10^{-4}$ **Figure 2B**), but RF surround diameter was not significantly affected by feedback inactivation (*control* vs *laser* 4.71 ± 0.43º vs 5.38 ± 2.77º, $p_{bootstrap} = 0.15$, **Figure 2C**). Feedback inactivation increased RF diameter in all layers (*control* vs *laser;* SG 1.23 ± 0.11º vs 1.53 ± 0.10º; L4C 1.31 ± 0.17º vs 2.26 ± 0.35º; IG 1.29 ± 0.25º vs 1.88 ± 0.26º, $p_{bootstrap} < 0.04$) but did not significantly affect the surround size (SG 4.90 ± 0.62 vs 6.11 ± 0.85º; L4 5.63 ± 1.10º vs 6.16 ± 0.90º; 4.25 ± 0.70º vs 4.35 ± 0.70º, $p_{bootstrap} > 0.16$). In approximately half of the cells, feedback inactivation increased maximum spike-rate.

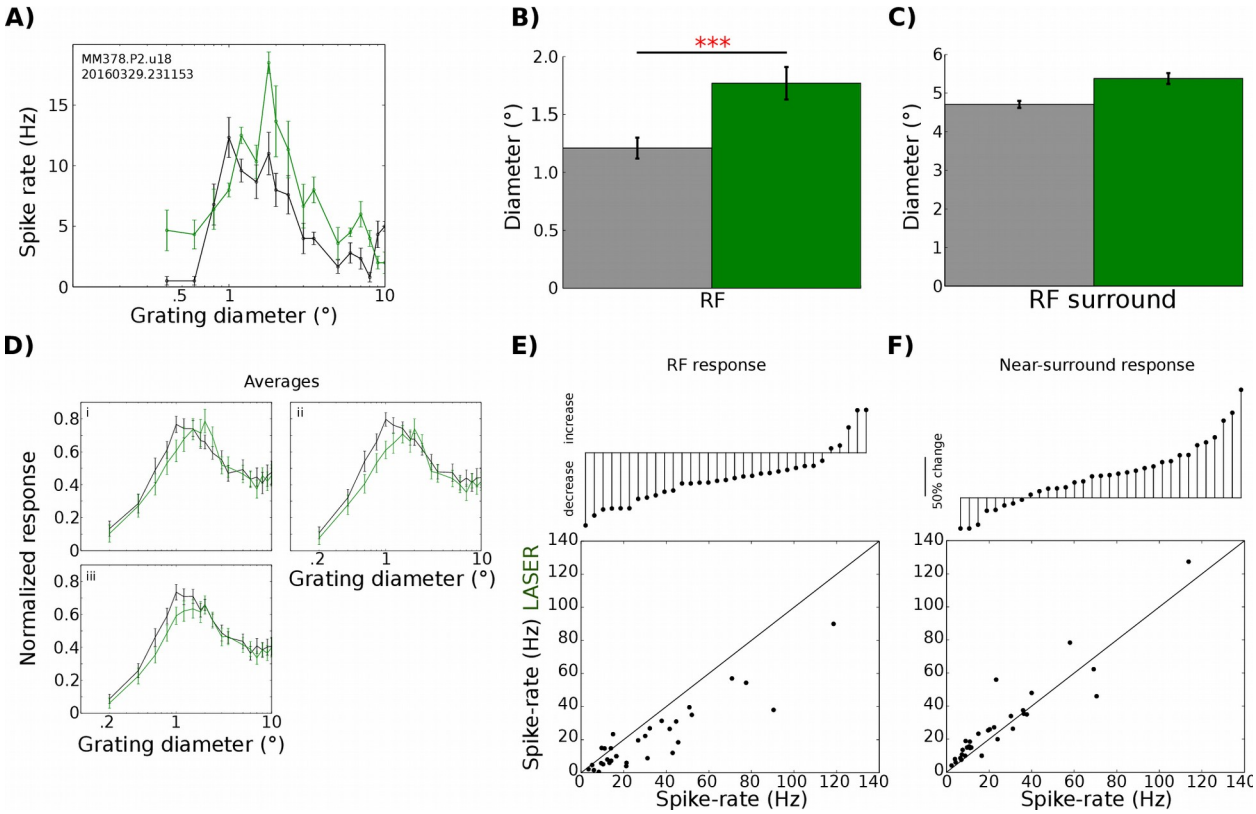

Figure 2. **Feedback excites RF center and suppresses RF surround.** **A)** An example cell demonstrating decreased response when the stimulus is confined to the RF center (peak of the control curve, black), increased RF size (shift in the peak of the curve measured with the laser on, green), and released surround suppression (increased response at stimulus diameters at which the control curve is already decreasing). **B)** RF size (defined as the peak of the curve) without (grey) and with (green) the laser stimulation. **C)** RF surround size (smallest stimulus size at which the response is within 5% of the response at the largest stimulus). **D)** Averages over i) cells showing increase in RF size and peak response ii) cells showing increase in RF size iii) all cells significantly modulated by the laser. **E)** Feedback inactivation reduces responses at RF. top) percentage response change caused by the laser stimulation when the stimulus is confined to the RF. Downward and upward stems indicate decreased and increased response, respectively. The scale bar shows 50% change in response. bottom) Spike-rates to stimulus covering the RF. **F)** Feedback inactivation increases responses at RF near-surround. Conventions as in E.

bioRxiv preprint doi: https://doi.org/10.1101/094680; this version posted December 16, 2016. The copyright holder for this preprint (which was not certified by peer review) is the author/funder, who has granted bioRxiv a license to display the preprint in perpetuity. It is made available under aCC-BY-NC-ND 4.0 International license.

Feedback from V2 controls visual responses of V1 neurons via two distinct mechanisms; excitation to the RF center and suppression via RF surround. Inactivating feedback strongly reduced spike-rates to stimuli within the RF center (mean spike-rate reduction 32.0 ± 6.03% $p_{bootstrap} < 10^{-5}$; *control* vs *laser*; 43.8 ± 14.1 spks/s vs 35.1 ± 15.3 spks/s, **Figure 2E**) and significantly increased responses (release from suppression) to stimuli covering the RF and RF near-surround (mean spike-rate increase 29.2 ± 7.14% $p_{bootstrap} < 10^{-5}$; *control* vs *laser;* 36.4 ± 12.3 spks/s vs 43.5 ± 17.2 spks/s, **Figure 2F**). There was a moderate but statistically insignificant relationship between response reduction and change in RF diameter when feedback was inactivated (Pearson's correlation (r) = -0.31, p=0.11), as well as between change in RF diameter and release from surround suppression (r = 0.32, p=0.08). We have previously shown that the visuotopic extent of V2 feedback to V1 is coextensive with the diameter of the RF near-surround of V1 neurons [11, 12]. Consistent with this, inactivating feedback from V2 did not produce significant changes in response to stimuli covering both the RF near and far-surround (mean spike-rate increase 7.10 ± 13.4%, $p_{bootstrap} = 0.28$; *control* vs *laser;* 20.9 ± 8.71 spks/s vs 19.79 ± 7.69 spks/s).

Inactivation of axons terminals using Arch may facilitate synaptic transmission with prolonged light pulses, while Arch is consistently suppressive at 200ms pulse width [13]. Thus, we repeated our analysis by focusing only on the first 200ms of the response. We found no qualitative differences between the original analysis and the short time-scale analysis. Consistent with the original analysis, the RF size showed a striking increase in its diameter when feedback was inactivated (*control* vs *laser*; 1.14 ± 0.07º vs 1.67 ± 0.24, $p_{bootstrap} = 0.02$, 19 units producing reliable response within the initial 200ms were analyzed), responses to stimuli confined to the RF were significantly reduced (mean spike-rate reduction 45.1 ± 8.62% $p_{bootstrap} < 10^{-5}$; *control* vs *laser* 26.1 ± 8.89 spks/s vs 21.6 ± 10.3 spks/s) and responses to stimuli covering the RF and RF near-surround significantly increased (mean spike-rate increase, 67.6 ± 34.0 % $p_{bootstrap} = 0.03$). Feedback inactivation did not produce significant changes when the stimulus covered both the near and the far-surround (mean spike-rate increase, 14.0 ± 19.7%; *control* vs *laser;* 11.67 ± 6.27 spks/s vs 13.25 ± 7.71 spks/s). This confirms that the laser induced effects reflect suppressed, instead of facilitated, feedback from V2.

Specific optogenetic inactivation has allowed us to resolve the controversy over whether V2 feedback causes general amplification or surround modulation of V1 responses [1-4, 14, 15]. A large proportion of neurons (~36%) showed reduced surround modulation or increased RF size at low laser irradiance, but generally reduced response at high irradiance (**Figure 3A, G**). At the irradiance producing the largest general suppression, the RF diameter was significantly smaller when feedback was intact (1.19 ± 0.11º) compared to when feedback was inactivated (1.60 ± 0.14º, $p_{bootstrap} = 0.013$, **Figure 3B**) but RF surround size was not significantly affected (*control* vs *laser*; 4.48 ± 0.43º vs 4.07 ± 0.53º, $p_{bootstrap} = 0.23$, **Figure 3C**). Spike-rates were significantly reduced to stimuli covering only the RF (mean spike-rate reduction 54.4 ± 3.99% $p_{bootstrap} < 10^{-5}$; *control* vs *laser* 53.1 ± 9.26 spk/s vs 21.8 ± 3.01 spk/s, **Figure 3E**) as well as to stimuli covering the RF and the near-surround (mean spike-rate reduction 28.3 ± 6.14%, $p_{bootstrap} < 10^{-5}$; *control* vs *laser* 43.1 ± 9.07 spk/s vs 26.5 ± 4.12 spk/s, **Figure 3F**) as well as RF far-surround (mean spike-rate reduction 33.2 ± 8.27%, $p_{bootstrap} < 10^{-5}$; *control* vs *laser* 13.3 ± 3.27 spk/s vs 7.12 ± 1.38 spk/s). We considered several properties that may separate these cells from the cells not showing general suppression (layer, surround suppression, spike-width, maximum spike-rate, baseline,

bioRxiv preprint doi: https://doi.org/10.1101/094680; this version posted December 16, 2016. The copyright holder for this preprint (which was not certified by peer review) is the author/funder, who has granted bioRxiv a license to display the preprint in perpetuity. It is made available under aCC-BY-NC-ND 4.0 International license.

trial-by-trial variability), and found that these cells had stronger surround suppression (SI 78.0 ± 3.05% vs 49.0 ± 7.13%, $p_{bootstrap} < 10^{-5}$) and while statistically insignificant ($p_{bootstrap} = 0.06$), they were most prevalent in supragranular layers (**Figure 3D**). Notably, the effective irradiance in supragranular layers is higher compared to the other layers, and we hypothesize that were we able to deliver high enough irradiance to the infragranular layers, without damaging the supragranular layers, larger proportion of cells would show general suppression. That feedback inactivation both reduces surround suppression and response gain depending on the inactivation level suggests that previous studies were most likely targeting feedback with different intensity and thus found conflicting results.

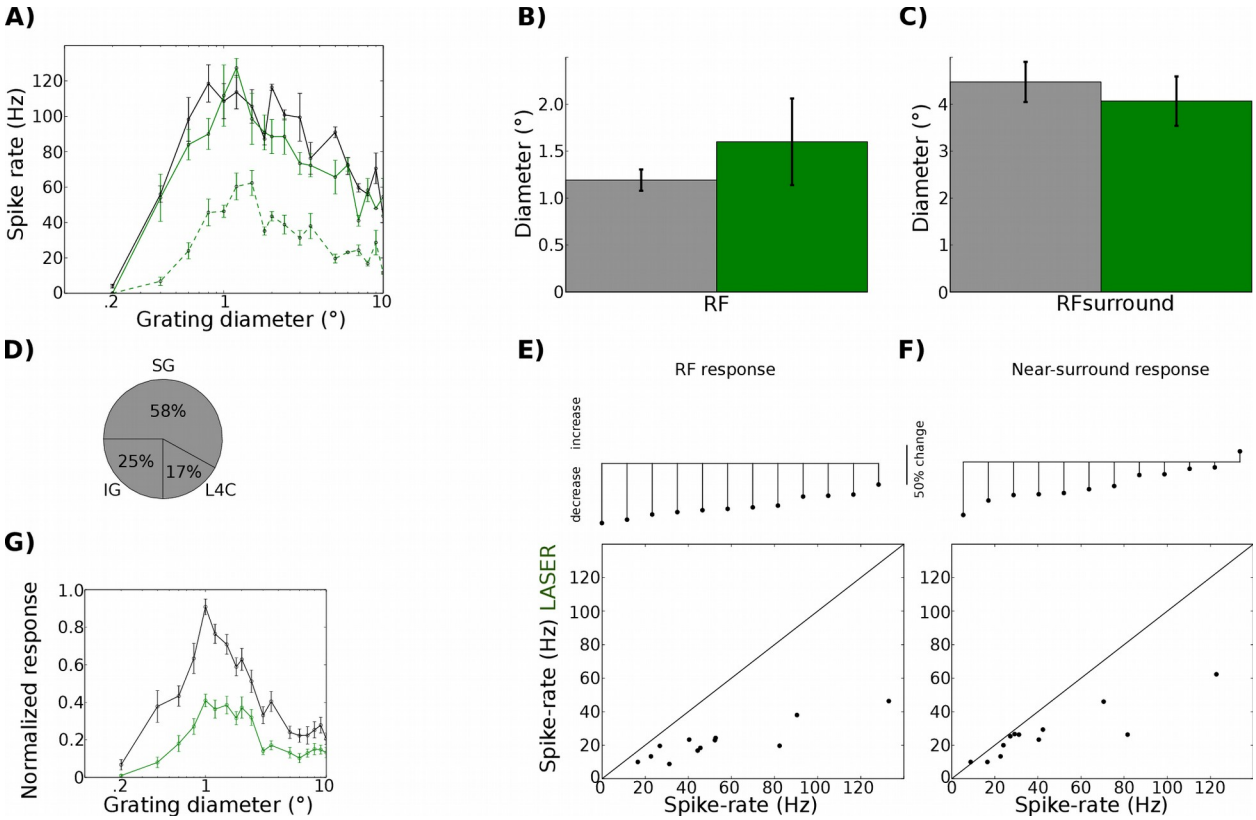

Figure 3. <u>Feedback controls the overall gain of V1 responses.</u> A) An example cell demonstrating increased RF size at low irradiance, and general suppression at high irradiance. **B)** Average RF size for the population of cells showing general suppression. **C)** Average RF surround size for the population of cells showing general suppression. **D)** Distribution of cells showing general suppression across layers. **E)** Feedback inactivation reduces responses at RF. top) percentage response change caused by the laser stimulation when the stimulus is confined to the RF. Downward and upward stems indicate decreased and increased response, respectively. The scale bar shows 50% change in response. bottom) Spike-rates to stimulus covering the RF. **F)** In contrast to feedback inactivation at low irradiance, feedback inactivation at high irradiance decreases responses at RF near-surround. Conventions as in E. **G)** Average.

DISCUSSION

Establishing a causal link between response properties of cortical neurons and components of the neural circuit embedding them is a central challenge in modern neuroscience. This study provides a comprehensive picture of how cortico-cortical feedback regulates visually driven neural activity in the primate visual cortex. By targeting optogenetic inactivation specifically and selectively to the feedback pathways terminating in the primary visual cortex, this study has resolved the controversies regarding how feedback regulates contextual modulation and the

bioRxiv preprint doi: https://doi.org/10.1101/094680; this version posted December 16, 2016. The copyright holder for this preprint (which was not certified by peer review) is the author/funder, who has granted bioRxiv a license to display the preprint in perpetuity. It is made available under aCC-BY-NC-ND 4.0 International license.

overall response gain of visual neurons. We have demonstrated that even the most fundamental response properties of cortical neurons, such as the receptive field size, can be modulated by feedback signals. Given the similarity between human and non-human primate brain, this study represents a step forward in the understanding of cortico-cortical feedback, and thus provides insight into the potential for therapeutic intervention for conditions arising from pathological communication between cortical areas.

bioRxiv preprint doi: https://doi.org/10.1101/094680; this version posted December 16, 2016. The copyright holder for this preprint (which was not certified by peer review) is the author/funder, who has granted bioRxiv a license to display the preprint in perpetuity. It is made available under aCC-BY-NC-ND 4.0 International license.

REFERENCES

1. Hupé, J.M., et al., *Cortical feedback improves discrimination between figure and background by V1, V2 and V3 neurons.* Nature, 1998. **394**: p. 784-787.
2. Sandell, J.H. and P.H. Schiller, *Effect of cooling area 18 on striate cortex cells in the squirrel monkey.* J. Neurophysiol., 1982. **48**: p. 38-48.
3. Hupé, J.M., et al., *Response modulations by static texture surround in area V1 of the macaque monkey do not depend on feedback connections from V2.* J. Neurophysiol., 2001. **85**: p. 146-163.
4. Nassi, J.J., S.G. Lomber, and R.T. Born, *Corticocortical feedback contributes to surround suppression in V1 of the alert primate.* J. Neurosci., 2013. **33**(19): p. 8504-17.
5. Han, X., et al., *A high-light sensitivity optical neural silencer: development and application to optogenetic control of non-human primate cortex.* Front Syst Neurosci, 2011. **5**: p. 18.
6. Grinvald, A., et al., *Functional architecture of cortex revealed by optical imaging of intrinsic signals.* Nature, 1986. **324**(6095): p. 361-4.
7. Federer, F., et al., *Four projection streams from primate V1 to the cytochrome oxidase stripes of V2.* J Neurosci, 2009. **29**(49): p. 15455-71.
8. Kadir, S.N., D.F. Goodman, and K.D. Harris, *High-dimensional cluster analysis with the masked EM algorithm.* Neural Comput, 2014. **26**(11): p. 2379-94.
9. Rossant, C., et al., *Spike sorting for large, dense electrode arrays.* Nat Neurosci, 2016. **19**(4): p. 634-41.
10. Stujenske, J.M., T. Spellman, and J.A. Gordon, *Modeling the Spatiotemporal Dynamics of Light and Heat Propagation for In Vivo Optogenetics.* Cell Rep, 2015. **12**(3): p. 525-34.
11. Angelucci, A. and P.C. Bressloff, *The contribution of feedforward, lateral and feedback connections to the classical receptive field center and extra-classical receptive field surround of primate V1 neurons.* Prog. Brain Res., 2006. **154**: p. 93-121.
12. Angelucci, A., et al., *Circuits for local and global signal integration in primary visual cortex.* J. Neurosci., 2002. **22**: p. 8633-8646.
13. Mahn, M., et al., *Biophysical constraints of optogenetic inhibition at presynaptic terminals.* Nat Neurosci, 2016. **19**(4): p. 554-6.
14. Bardy, C., et al., *"Top-down" influences of ispilateral or contralateral postero-temporal visual cortices on the extra-classical receptive fields of neurons in cat's striate cortex.* Neurosci., 2009. **158**: p. 951-968.
15. Wang, C., et al., *Influence of 'feedback' signals on spatial integration in receptive fields of cat area 17 neurons.* Brain Res., 2010. **1328**: p. 34-48.